Published in final edited form as:
Neuron. 2009 July 16; 63(1): 48–62. doi:10.1016/j.neuron.2009.06.006.

Fgf10 regulates transition period of cortical stem cell differentiation to radial glia controlling generation of neurons and basal progenitors

Setsuko Sahara and **Dennis D. M. O'Leary**[1]
Molecular Neurobiology Laboratory, The Salk Institute, 10010 N. Torrey Pines Rd., La Jolla, CA 92037

Summary

Radial glia (RG), the progenitors of cortical neurons and basal progenitors (BPs), differentiate from neuroepithelial cells (NCs) with stem cell properties. We show that the morphogen, Fgf10, is transiently expressed by NCs coincident with the transition period of NC differentiation into RG. Targeted deletion of Fgf10 delays RG differentiation, whereas overexpression has opposing effects. Delayed RG differentiation in Fgf10 mutants occurs selectively in rostral cortex, paralleled by an extended period of symmetric NC divisions increasing progenitor number, coupled with delayed and initially diminished production of neurons and BPs. RG eventually differentiate in excess number and overproduce neurons and BPs rostrally resulting in tangential expansion of frontal areas and increased laminar thickness. Thus, transient Fgf10 expression regulates timely differentiation of RG, and through this function, determines both length of the early progenitor expansion phase and onset of neurogenesis, and ultimately the number of progenitors and neurons fated to specific cortical areas.

Keywords

arealization; cortical lamination; neuroepithelial cells; neurogenesis; Notch; symmetric divisions; asymmetric divisions; cortical size

1**Corresponding author:** Dennis D. M. O'Leary, Molecular Neurobiology Laboratory, The Salk Institute, 10010 N. Torrey Pines Rd., La Jolla, CA 92037, doleary@salk.edu, FAX: 858-558-6207, Tel: 858-453-4100 ext 1415.

COMPETING INTERESTS
The authors have no competing financial or non-financial interests related to this work.

The neocortex is responsible for sensory perception and complex cognitive tasks. Corticogenesis can be divided into sequential phases, beginning with an expansion phase characterized by cortical stem cells that undergo symmetric division to expand their number, followed by their differentiation into a mature progenitor, radial glia, and finally neurogenesis during which radial glia produce cortical neurons. We show that Fgf10 regulates the timely differentiation of radial glia, and through this function, determines the timing and length of key phases of corticogenesis, the number of radial glia and neurons produced, and as a consequence cortical size, laminar thickness, and area patterning. Thus, Fgf10 serves a central, fundamental role in corticogenesis through its regulation of cortical stem cell differentiation and by determining the selective expansion of specific cortical areas, Fgf10 can emphasize the specialized functions attributed to them.

Introduction

Early in corticogenesis, cortical progenitors referred to as neuroepithelial cells (NCs), have stem cell properties and expand their numbers within the ventricular zone (VZ) by symmetric cell division that produces two like progenitors. Later, NCs differentiate into a mature progenitor termed a radial glia (RG) that exhibits asymmetric division to produce a pair of unlike cells comprised of an RG to maintain the proliferative pool and either a deep layer cortical neuron or a basal progenitor (i.e. intermediate progenitor) that establishes the subventricular zone (SVZ) and later produces superficial layer cortical neurons (Gotz and Huttner, 2005). Little is known about the mechanisms that mediate this critical transition period that bridges the early expansion phase characterized by symmetric division of NCs with the later neurogenic phase characterized by asymmetric division of RG. However, the timing of the transition from NE to RG has critical implications for corticogenesis because models predict that minor changes in the proportion of progenitors exhibiting one or the other division mode at early stages result in substantial changes in the number of progenitors and ultimately cortical size (Caviness et al., 1995; Rakic, 1995). These predictions are supported by the analysis of mice genetically-modified to express a stabilized form of β-catenin, which regulates the mode of cell division and leads to an increase in symmetric divisions producing progenitors (Chenn and Walsh, 2002), and mice with a deletion of either caspase-9 or Cpp32, which reduces apoptotic cell death among progenitors (Chenn and Walsh, 2002; Kuida et al., 1998; Kuida et al., 1996). Each of these genetic manipulations results in an increase in cortical progenitors, and presumably as a result, an increase in cortical size.

Most, if not all, neurons generated in the cortical VZ are progeny of BLBP-positive RG that differentiate from BLBP-negative NCs (Anthony et al., 2004). Although NCs may produce a small proportion of neurons (Gotz and Huttner, 2005), within the cortex they are primarily cortical stem cells that divide symmetrically to produce two like cells, expanding the progenitor pool before differentiating into BLBP-positive RG. Therefore, the differentiation of NCs into RG is a critical step in determining whether progenitors retain a symmetric mode of cell division that serves to expand progenitor pools or acquire an asymmetric mode to populate the cortex.

Notch signaling is involved in the transition of NCs into RG. For example, Notch1 promotes RG identity when an activated form is overexpressed before the onset of neurogenesis (Gaiano et al., 2000) and BLBP expression is diminished in mice deficient for both Notch1 and Notch3 in the forebrain (Anthony et al., 2005). However, Notch signaling is not the only determinant for RG differentiation because BLBP expression is not entirely abolished in Notch1 and Notch3 double knockout mice. Fibroblast growth factor (Fgf) signaling is also implicated in the differentiation of NCs into RG. For example, in vivo studies based upon expressing a constitutively active form of the Fgf receptor, Fgfr2, indicate that its activation in NCs promotes their differentiation into RG (Yoon et al., 2004). In contrast, though, in vitro studies of dissociated cortical cell cultures indicate that Fgfr1 and Fgfr3 promote the proliferation of cortical NCs, a function distinct from differentiation (Maric et al., 2007). Thus, these findings indicate that the different Fgf receptors expressed by cortical NCs have distinct effects on their proliferation and differentiation.

Fgf receptors expressed by cortical NCs are activated by unique subsets of Fgfs. Several Fgfs influence corticogenesis, but only Fgf2 has been reported to be expressed in the cortical VZ. Fgf2 is expressed by progenitors throughout the cortical VZ and deletion of it results in diminished proliferation of progenitors (Vaccarino et al., 1999). Fgf8, Fgf17, and Fgf18 are expressed in the anterior neural ridge (ANR) / commissural plate (CoP) positioned at the anterior midline of the nascent neocortex. Fgf2 and Fgf8, which have been most studied, preferentially function through Fgfr1, Fgfr2c and Fgfr3, and contribute to the proliferation and survival of cortical progenitors (Gutin et al., 2006; Maric et al., 2007; Ornitz et al., 1996).

Fgf15, which has a very dynamic expression pattern in forebrain, indirectly influences proliferation in cortex through its regulation of Fgf8 in the CoP (Borello et al., 2008). Finally, Fgf7 is expressed in the anti-hem, a putative patterning center positioned along the rostral-caudal cortical axis at the border between dorsal telencephalon (dTel) and ventral telencephalon; Fgf7 preferentially binds Fgfr2b but to date it has not been assigned a function in corticogenesis (Assimpopolous et al., 2003). Thus, progress has been made on defining Fgfs responsible for regulating proliferation of cortical progenitors, but Fgfs responsible for promoting the differentiation of NCs into RG remain vague.

Here we show that Fgf10, a high affinity ligand for Fgfr2b, controls RG differentiation in the cortical VZ and through its regulation of this process has critical consequences for corticogenesis and patterning. The present study is based upon our analysis of expression patterns of each of the twenty-two members of the Fgf family, which reveal that Fgf10 has a particularly novel expression pattern suggestive of a prominent and unique role in corticogenesis. We find that Fgf10 is transiently expressed by cortical progenitors during the transition period coincident with the differentiation of NCs into RG. These findings prompted us to investigate the role of Fgf10 in this differentiation process and the consequences of altering Fgf10 expression on corticogenesis. We find that Fgf10 drives the timely differentiation of NCs into RG and through this function determines both the length of the expansion phase of NCs and the onset of neurogenesis. The generation of neurons and BPs, both the progeny of RG, is similarly effected by deletion of Fgf10, with each showing an initial delay and decrease in production followed by an increase. Thus, our findings demonstrate that through its regulation of RG differentiation, Fgf10 determines the size of progenitor pools both within the VZ and the SVZ, with significant consequences for neuronal production, and ultimately the size of the cortex as well as its laminar and area patterning.

RESULTS

Fgf10 is transiently expressed in apical VZ during transition period of corticogenesis

We analyzed Fgf expression in embryonic dTel and found that Fgf10 has a unique expression pattern that suggests a role in corticogenesis (Figure 1). Previous studies have shown that Fgf10 is expressed in early forebrain, with strong expression in infundibulum in ventral hypothalamus (Bachler and Neubuser, 2001;Treier et al., 2001), but expression in dTel has not been reported. Therefore we analyzed in detail Fgf10 expression using in situ hybridization on sections of E9.5 to E16.5 telencephalon (Figure 1 and data not shown). Fgf10 expression is first detected at E9.5, but is weak and is limited to the anterior midline of dTel (Figure 1A and A'). At E10.0 to E10.5, Fgf10 expression becomes evident at the apical side of the entire VZ of dTel (Figure 1B, C, B' and C') and is sustained through E11.5 (Figure 1D and D'), after which it decreases in intensity, becoming undetectable by E13.5 (Figure 1E and E'). In summary, Fgf10 is transiently expressed in cortical progenitors at the apical side of the VZ during the transition period when NCs differentiate into RG, signaling the onset of the neurogenic phase. The restricted localization of Fgf10 transcripts suggest that Fgf10 is expressed by NCs at a specific stage of differentiation, most likely M phase.

Fgf10 promotes RG differentiation

Our findings indicate that Fgf10 is expressed in progenitors during the period that they differentiate from NCs into RG, which go on to produce neurons and BPs, and subsequently glia (Anthony et al., 2004; Malatesta et al., 2003). To address whether Fgf10 influences the differentiation of RG from NCs, we analyzed the expression of the RG-specific markers BLBP and GLAST in the cortex of Fgf10 −/− mice compared to wild type (wt) using specific antibodies (Hartfuss et al., 2001). Previous studies have reported that BLBP expression can be detected using immunostaining at E12.5 (Anthony et al., 2004). Therefore we analyzed mice

between E10.5 and E13.5. We find no detectable staining in the cortex of either wt or Fgf10 −/− mice at E10.5 (data not shown). However, by E11.5, we readily detect BLBP in wt mice with the strongest immunostaining in ventrolateral and dorsomedial cortex (Figure 2A) and mild expression in dorsolateral cortex (Figure 2A, D). In wt, BLBP immunostaining is stronger and more extensive in the cortex at E12.5 (Figure 2B, E). In contrast, BLBP immunostaining in the cortex of Fgf10 −/− mice is deficient relative to wt (compare Figures 2A, B, D, and E to 2A',B', D' and E'). By E13.5, BLBP immunostaining is found throughout the cortical VZ in wt, and in contrast to earlier stages, immunostaining for BLBP in Fgf10 −/− cortex at E13.5 is indistinguishable from wt (compare Figure 2C and C').

Immunostaining for GLAST corroborates our findings with BLBP. We find that GLAST immunostaining is more modest than that for BLBP during the transition period and is most detectable in lateral cortex (Figure 2F). Like BLBP, GLAST is also downregulated in Fgf10 −/−cortex (Figure 2F'). We conclude from these findings that Fgf10 is required for the differentiation of NCs into RG.

In addition to the induction of RG markers, we also examined within the VZ the expression of Occludin, a tight-junction marker localized to the surfaces of NCs, particularly their apical surface near the lumen of the lateral ventricle, that is characteristically downregulated as they differentiate into RG (Aaku-Saraste et al., 1996). At E11.5, we observe strong expression of Occludin at the apical surface of the VZ in the cortex of both wt and Fgf10−/− mice (Figure S1A, A'). This expression is strongly diminished by E12.5 in wt cortex (Figure S1B, C), whereas in contrast, in Fgf10−/− mice it is diminished in caudal cortex at E12.5 but is aberrantly sustained in rostral cortex (Figure S1B', C', E). By E13.5, Occludin expression is downregulated throughout the cortex of Fgf10 −/− mice and resembles wt (Figure S1D, D'). Thus, downregulation of the expression of the tight-junction marker Occludin that occurs throughout wt cortex between E11.5 and E12.5 is delayed selectively in rostral cortex of Fgf10 −/− mice, which correlates both spatially and temporally with the delay in upregulation of the expression of the RG markers BLBP and GLAST. These complementary sets of findings indicate that the deletion of Fgf10 delays the differentiation of RG from NCs in vivo.

To test whether Fgf10 is sufficient to promote RG differentiation, we performed gain-of-function experiments by overexpressing Fgf10 using in utero electroporation. An expression vector with Fgf10 under the control of the CAG promoter was co-electroporated at E11.5 with an EGFP expression vector as a reporter to reveal the electroporation domains in the brains analyzed at E12.5. BLBP immunostaining in control vector-electroporated domains is identical to unelectroporated brains (n=3, Figure 3B, C, E, F and data not shown). In contrast, when Fgf10 is overexpressed, we find a higher level of BLBP immunostaining coincident with the ectopic domain of Fgf10 expression (n=3, Figure 3B', C', E', and F'). In summary, our gain-of-function analyses indicate that Fgf10 is sufficient to promote the differentiation of NCs into RG, whereas our loss-of-function analyses show that Fgf10 is required for the appropriate timing of this differentiation event.

The loss of Fgf10 delays RG differentiation in rostral dTel

As described above, Fgf10 expression is first detected in rostral cortex, and then expands caudally (Figure 1A and B). Therefore, we speculated that the diminished expression of BLBP that we observe in Fgf10−/− cortex compared to wt may also be graded, resulting in a more pronounced effect on RG differentiation in rostral cortex. To address this issue, we compared the expression of BLBP across the rostral-caudal cortical axis in Fgf10 −/− mice to their wt littermates at E11.5. Qualitatively, we find that BLBP immunostaining is substantially diminished rostrally in mutant cortex compared to wt, but that caudally the staining is similar (Figure 4A and A'). This impression is corroborated by quantification of fluorescence intensity of the BLBP immunostaining at five positions along rostral-caudal cortical axis (Figure 4B).

Thus, BLBP expression is significantly diminished in rostral cortex of Fgf10 mutants compared to wt.

To extend these findings, we performed two additional quantitative analyses of cortical BLBP expression in wt and Fgf10 −/− littermates. First, we measured overall intensity of the fluorescence immunostaining at a mid-rostral level and find that relative to wt, the staining in Fgf10 −/− cortex is diminished by 82% at E11.5 and 57% at E12.5, whereas the staining intensity is comparable in wt and mutant cortex at E13.5 (Figure 4C, n=4). To address this issue at a cellular level, we dissociated, plated and immediately immunostained cells from the rostral half of the cortex of wt and Fgf10 −/− littermates at E11.5, E12.5 and E13.5 (Figure 4D–F). At E11.5, 30% of wt cortical cells are BLBP positive, whereas only 10% of cells from Fgf10 −/− cortex are BLBP positive (Figure 4F). At E12.5, 49% of cells are BLBP positive in wt cortex, compared to only 28% in Fgf10 −/− cortex (Figure 4F). By E13.5, 48% of wt cortical cells are BLBP positive, compared to 52% in Fgf10 −/− cortex (Figure 4F). These data show a 67% decrease in the percentage of cells that are BLBP positive in Fgf10 −/− cortex compared to wt at E11.5, and a 42% decrease at E12.5. To restate this data, in the presence of Fgf10, we observe a 300% increase in VZ cells that are BLBP positive at E11.5 and a 175% increase at E12.5. By E13.5, BLBP immunostaining is virtually indistinguishable between wt and Fgf10 −/− cortex.

These quantitative data indicate that in wt cortex, BLBP expression progressively increases between E11.5 and E13.5, both in overall intensity and in the proportion of VZ cells expressing BLBP, overlapping with the transient expression of Fgf10. However, this progressive increase in BLBP immunostaining is delayed and transiently diminished in rostral cortex of Fgf10 −/− mutants, but that by E13.5, when Fgf10 expression is normally down-regulated in wt cortex, BLBP staining in Fgf10 −/− cortex has increased and is comparable to wt. Thus, Fgf10 expression by NCs is required for their timely differentiation into RG in rostral cortex during the transition period.

Early production of neurons and BPs is delayed and diminished in Fgf10 rostral mutant cortex

Our findings indicate that Fgf10 controls the differentiation of NCs into RG, and that in the absence of Fgf10, this differentiation process is delayed. We predicted a similar delay in the production of the earliest generated neurons and BPs by differentiated RG. To address this issue, we used specific markers to compare wt and Fgf10 −/− mice beginning at E10.5, when preplate neurons are first generated, through to E14.5, encompassing the period when neurons that will form layers 5 and 6 of the cortical plate are generated.

Cortical preplate neurons, which arise from BLBP-positive RG (Anthony et al., 2004), are generated between E10.5 and E12.5 and are uniquely marked by the T-box transcription factor, Tbr1 (Hevner et al., 2001). In E10.5 wt mice, a low density of Tbr1-positive neurons forms the nascent preplate just beneath the pial surface (Figure 5A). In Fgf10 −/− mice, we find a significant reduction in the number of Tbr1-positive neurons in rostral cortex compared to wt littermates (compare Figure 5A to 5A', and G). In contrast to wt, sections through rostral cortex of Fgf10 −/− mice have at most only one Tbr1-positive neuron, many have none. We continue to observe a significant reduction in the number of Tbr1-positive neurons at E11.5, with 83% fewer in the rostral cortex of Fgf10 −/− mice compared to wt littermates (Figure 5B, B', and G, n=4). The difference in the numbers of Tbr1-positive neurons found in Fgf10 −/− cortex compared to wt is less significant at E12.5, the last day of significant production of preplate neurons in wt, following which RG generate cortical plate neurons. This trend continues over the next two days with the Tbr-1 positive cortical plate of the Fgf10 −/− mice coming to more closely resemble that in wt (Figure 5D–E', and G). We confirmed the reduction in numbers of preplate neurons at E12.5 by TuJ1 immunostaining, which labels type III beta tubulin

characteristic of all postmitotic neurons, and reveals a significant reduction in neuronal density in Fgf10 −/− cortex (Fig. 5F and 5F'). In conclusion, in Fgf10 −/− mice, cortical neurogenesis lags behind wt by about a day and a half to two days, a delay similar to that observed in the differentiation of their RG progenitors.

We also analyzed the generation of BPs, which arise from RG and form the SVZ, a second germinal zone outside of the VZ that produces superficial layer neurons. For this analysis, we performed immunostaining from E11.5 through E17.5 using a marker specific for BPs, the T-box transcription factor Tbr2 (Englund et al., 2005) (Figure S2). We find a significant reduction of BPs in Fgf10−/− cortex compared to wt littermates at E11.5 and E12.5 (Figure S2A, B, A' and B', n=4, 42% reduction for E11.5, 40% for E12.5). In contrast, at E13.5, the number of BPs is the same in Fgf10 −/− cortex as in wt, but between E14.5 and E17.5, we find a trend toward an increase in BPs, with the difference being statistically significant at E15.5 (Figure S2H). These findings indicate that the delay in the differentiation of NCs into RG within the cortical VZ is accompanied not only by a delayed onset of the production of neurons, but also by a diminished production of BPs. However, as for neurons, at later stages, production of BPs is increased in Fgf10 −/− cortex compared to wt.

Delayed differentiation of NCs into RG in Fgf10−/− mutants results in over-production of progenitors in rostral cortex

Our findings above show that the differentiation of NCs into RG in the VZ is delayed in rostral Fgf10 −/− cortex and is paralleled by a delay and reduction in both early neurogenesis and the initial production of BPs. We carried out additional analyses to assess potential implications of these findings. We first addressed whether the delay in RG differentiation and / or the Fgf10 deficiency results in a defect that alters cell cycle kinetics or survival of progenitors in the cortical VZ. Our analyses though indicate that the length of the cell cycle measured with the thymidine analog, BrdU, and apoptotic cell death revealed by immunostaining for activated Caspase 3, are indistinguishable between wt and Fgf10 −/− mice (Figure S3).

To address whether the delay in RG differentiation may affect the mode of cell division of progenitors, we first examined the ratio of cells that exit or re-enter the cell cycle at early stages of neurogenesis. We exposed proliferating cells to a pulse of BrdU at E11.5 and 24 hrs later fixed the mice and immunostained for Ki67 to mark actively proliferating cells. Cells that are singly labeled with BrdU have exited the cell cycle over the 24 hr period to become preplate neurons (Takahashi et al., 1999), whereas those that are double labeled with BrdU and Ki67 are proliferating progenitors. We find that in rostral cortex, 66% fewer progenitors exit the cell cycle by E12.5 in Fgf10 −/− mice compared to wt (Figure 6A, A' and B, n=4, $p<0.05$). This result indicates that in Fgf10 −/− cortex, at early stages of cortical neurogenesis, progenitors are more likely to remain in the proliferative mode than exit it and become neurons. This finding provides a mechanism to account for the reduced number of preplate neurons in Fgf10 −/− cortex compared to wt, and is consistent with the delayed differentiation of NCs into RG in Fgf10 −/− cortex and the accompanying switch from symmetric to asymmetric division marking the onset of the neurogenic phase.

Our findings show that in Fgf10−/− cortex, progenitors remain in a mode of symmetric division for an extended period, resulting in the production of two progenitors when they divide, and exhibit a delay in becoming neurogenic and exhibiting asymmetric division. To address this issue, we examined the mode of cell division by following in vitro the fate of rostral cortical progenitors that were dissociated from E12.5 cortex and plated at clonal density; isolated individual cells were verified and followed over time (Figure 6C and D) (Qian et al., 1998). After 24 hours, cultured cells were immunostained with TuJ1 to selectively mark neuronal progeny to distinguish them from progeny that continue as progenitors, and each pair of daughter cells were scored (Figure 6C). We find a significant increase in symmetric divisions

of progenitors in rostral cortex of Fgf10 −/− mutants compared to wt, all of which produce two progenitors, typifying them as NCs (Figure 6D). Coincident with this change, the frequency of asymmetric divisions by progenitors is significantly decreased in rostral cortex of Fgf10 −/− mutants compared to wt. These significant changes in the division mode and output of progenitors in rostral cortex of Fgf10 mutants results in a selective expansion of the progenitor pool at early stages of corticogenesis compared to wt. This increased production of progenitors in Fgf10 −/− cortex occurs during an age that in wt coincides with the transition period when Fgf10 is transiently expressed and NCs differentiate into RG, and is consistent with both the delayed differentiation of NCs into RG and the concomitant delay in neuronal production in Fgf10 −/− cortex.

Based on these in vitro findings, we predicted an increase in progenitors in the rostral cortex of Fgf10 −/− mice compared to wt. To confirm this predicted increase, we used BrdU to label S-phase progenitors at E13.5 and E14.5 and analyzed the number of cells labeled in the cortical VZ one hour after BrdU exposure (Figure 7A, A', B, B', and Figure S4). We choose these ages because they are shortly after the stage that cortical Fgf10 expression ceases in wt, the differentiation of RG in Fgf10 mutants is indistinguishable from wt, and they are near the mid-point of cortical neurogenesis. Counts of BrdU labeled cells show a significant increase in the number of progenitors in rostral cortex of Fgf10 −/− mice compared to their wt littermates of 33% at E13.5 (Figure S4, n=4) and 40% at E14.5 (Figure 7C, n=4, $p<0.01$). To confirm the increase of progenitors in Fgf10−/− rostral cortex, we performed double immunostaining at E14.5 for the two types of neurogenic progenitors, using an antibody for the paired-box transcription factor Pax6 that marks RG and the Tbr2 antibody that marks BPs (Figure7D, D' and E). The number of Pax6 labeled cells exhibits a significant increase of 37%, similar to the 40% increase in numbers of progenitors determined using BrdU labeling of all proliferating cells. In summary, two independent methods of marking cortical progenitors confirm the in vitro prediction that the Fgf10 −/− mutant has an increased population of progenitors in the cortical VZ compared to wt.

Over-production of cortical progenitors and neurons in rostral cortex of Fgf10−/− mice results in a selective increase in laminar thickness and frontal areas

As described above, in Fgf10 −/− mice the differentiation of RG is preferentially delayed in rostral cortex, resulting in a lengthening of the expansion phase characterized by an increase in symmetric divisions that produce two progenitors, resulting in an increase in the progenitor pool within rostral cortex. Consistent with this expanded progenitor pool in rostral cortex, we find that the cortical hemisphere of Fgf10 −/− mice is significantly larger than that of wt littermates at P0 (Figure 8A – C). In addition, compared to wt, the radial thickness of the cortical wall in Fgf10 −/−mice is significantly increased selectively in rostral (frontal) cortex (Figure 8D and 8E), due largely to a 40% increase in the thickness of the cortical plate (Figure 8F, F', H, and I; $p<0.01$, n=8); in contrast, the thickness of caudal (occipital) cortex is virtually indistinguishable between mutant and wt (Figure 8D – I, n=8). Cell counts show that the increased thickness of the cortical plate in rostral cortex is due at least in part to a 33% increase in the number of cells in a radial traverse through it (Figure 8C, $p < 0.01$, n=4). In situ analysis at P0 (when the mutant dies) using the laminar-specific markers RORβ (predominantly marks layer 4; Figure S5B, B'), otx1 (predominantly marks layer 5; Figure S5C, C'), and Tbr1 (predominantly marks layer 6; Figure S5D, D'), suggests that layers that have been fully generated by birth in the Fgf10 −/− cortex (because of the delay in neurogenesis, generation of superficial layers is still ongoing at P0) are expanded to a roughly equal proportional extent in rostral cortex of Fgf10 −/− mice compared to wt. These findings suggest that the increased generation of neurons in the Fgf10 −/− cortex is made up of a roughly proportional increase in numbers of neurons of different laminar identities.

The cortical plate in the Fgf10 mutant exhibits a relatively uniform increase in thickness over the rostral half of the cortex (Figure 8) indicating that the increase in the numbers of cortical progenitors in the Fgf10 mutant has a similar uniformity over rostral cortex. We therefore addressed whether the increase in rostral cortical progenitors results in a preferential increase in the size of frontal cortical areas; if it does, we can conclude that area patterning information inherited by progenitors is fixed at early stages in corticogenesis, coincident with the transition period of differentiation of NCs into RG.

To address this issue, we performed a marker analysis of area size and patterning on P0 Fgf10 −/− mice and wt littermates. To analyze the size of frontal areas size, we first used whole mount in situ hybridization (WMISH) for cadherin8 (cad8), which selectively marks frontal/motor areas (Suzuki et al., 1997), and measured frontal area size. We find that the absolute size of the frontal Cad8 domain is expanded 63% compared to wt; importantly, even the relative size of the frontal cad8 domain is expanded by 45% in Fgf10−/− mutant, following correction for the 37% increase in overall cortical surface area in the Fgf10 mutant (Figure 9A–B, n=4). We also examined changes in area patterning by analyzing on sagittal sections through Fgf10 mutant and wt cortex the expression of Cad8 as well as other areal markers, including Lmo4, which marks borders between frontal/parietal cortex (i.e. frontal/motor with somatosensory areas) and parietal/occipital (somatosensory with visual areas) cortex (Bulchand et al., 2003), and ephrin-A5 (Figure 9E, E'), which is preferentially expressed in parietal (somatosensory) cortex (Mackarehtschian et al., 1999). Consistent with the cad8 WMISH, the caudal border of the Cad8 expression domain, which marks the frontal-parietal border, is shifted caudally, resulting in an increase in the frontal area domain. Similarly, we find that a similar border marked by Lmo4 and ephrin-A5 is also shifted caudally in the Fgf10 −/− cortex compared to wt. In contrast, the more caudal border (near the parietal-occipital junction) of each marker expression pattern remains relatively constant between Fgf10 mutant and wt cortex (Figure 9C–E'). These findings indicate that more rostral cortical areas, such as the frontal / motor areas, exhibit a preferential increase in the Fgf10 mutant compared to wt, whereas more caudal areas, such as visual, exhibit little significant change. Again these findings are consistent with a preferential expansion of the progenitor pool that gives rise to rostral (frontal) cortex, and indicates that area patterning information is fixed at the time the progenitor pools are expanded in the Fgf10 mutant cortex.

The size of frontal areas is regulated by the secreted morphogens Fgf8, Fgf17 and Fgf18, expressed in the CoP (Cholfin and Rubenstein, 2007; Fukuchi-Shimogori and Grove, 2001; Storm et al., 2006), in part by regulating in cortical progenitors the graded expression of transcription factors that specify area identities, such as Pax6, Emx2 and Coup-Tf1 (O'Leary et al., 2007; Sahara et al., 2007). Therefore, the increase in frontal areas in the Fgf10 mutant might be due to the Fgf10 deficiency resulting in changes in the expression of Fgfs expressed by the CoP or transcription factors that specify area identities within cortical progenitors. To address this issue, we used in situ hybridization to analyze the expression of these morphogens (Figure S6) early in corticogenesis, and find that the expression of each is indistinguishable between wt and Fgf10 mutants. Thus, we conclude that area identity is fixed at the time the excess progenitors are generated in the Fgf10 −/− cortex. Further, these findings indicate that Fgf10 expressed in the cortical VZ does not influence the expression of Fgfs in the CoP.

Discussion

In this study, we show that Fgf10 regulates the timely differentiation of NCs into RG, and through this function, determines the timing and length of key phases of corticogenesis, the size of cortical progenitor pools and neuronal number, and as a consequence cortical size, laminar thickness, and area patterning. Corticogenesis can be divided into a few sequential phases, beginning with the expansion phase characterized by NCs undergoing symmetric

divisions to expand the proliferative population, followed by the transition period during which NCs differentiate into RG, the neurogenic phase during which RG exhibit asymmetric divisions and generate neurons as well as basal progenitors, which themselves generate additional neurons, and finally the terminal phase during which progenitors undergo a terminal symmetric division and become quiescent.

We find that in mouse, Fgf10 is transiently expressed by progenitors in the VZ for two to three days beginning late in the expansion phase and continuing through the transition period during which NCs differentiate into RG. We used loss- and gain-of-function approaches to determine roles for Fgf10 in this differentiation process by analyzing mice with a targeted deletion of Fgf10 and the effect of in utero electroporation of Fgf10 expression constructs into the VZ. Fgf10 deletion causes a delay in the expression of markers for differentiated RG such as BLBP and GLAST and is complemented by a delay in the downregulation of a marker of NCs, Occludin, whereas overexpression of Fgf10 induces a significantly higher expression of BLBP. These results indicate that Fgf10 enhances the differentiation of NCs into RG and by its control of the timing of RG differentiation, Fgf10 determines both the end of the expansion phase and the beginning of the neurogenic phase. The delay in RG differentiation in Fgf10 mutants occurs preferably in rostral cortex and is paralleled by a comparable delay in neurogenesis and a lengthening of the phase of progenitor expansion within the cortical VZ through the symmetric division of NCs. This change is characterized by an increase in the proportion of progenitors that undergo symmetric divisions to produce two progenitors, a feature characteristic of NCs, at a stage during the transition period when asymmetric divisions to produce one progenitor and one neuron, a feature characteristic of RG, normally become predominant, resulting in a significant overproduction of progenitors in rostral cortex.

At early stages of neurogenesis, the production of both neurons and BPs is diminished in Fgf10 deficient cortex. However, when RG eventually differentiate, their numbers are significantly increased, subsequently resulting in an excess production of neurons and BPs, manifested by an increase in the radial thickness of the cortical plate as well as an increase in cortical surface area due primarily to a preferential increase in the size of frontal areas. These results demonstrate a central role for Fgf10 in controlling cortical neurogenesis by regulating the transition of NCs into RG, and through this regulatory process, determining the length of the phase of progenitor expansion exhibited by NCs. The bias of these functions of Fgf10 for rostral cortex implicates Fgf10 as a key regulator of the size of progenitor pools and neuronal number allocated to specific areas in the developing cortex.

The vertebrate family of Fgfs is comprised of twenty-two members, several of which have been reported to participate in cortical development, but our findings show that Fgf10 has unique functions distinct from these other Fgfs. Of these Fgfs, only Fgf10 and Fgf2 are expressed by progenitors in the cortical VZ. Whereas Fgf2 transcripts are broadly distributed over the VZ (Vaccarino et al., 1999), we find that Fgf10 transcripts are localized to the apical aspect of the VZ, resembling the labeling pattern obtained with JONES, an antibody against the 9-O-acetylated GD3, reported to mark early progenitors in the cortical VZ (Maric et al., 2007). This distinct localization of Fgf10 transcripts suggest that Fgf10 is expressed at a specific mitotic stage or by NCs at a specific stage of differentiation. Based upon our findings that Fgf10 enhances the differentiation of NCs into RG, we speculate that Fgf10 may be expressed as an NC undergoes its final symmetric division, promoting the differentiation of the daughter cells into RG.

Fgf2 has been reported to be a potent mitogenic factor for telencephalic progenitors in vitro (Murphy et al., 1990) and functions in this capacity by acting through Fgfr1 and Fgfr3 (Maric et al., 2007). Loss of Fgf2 results in a reduction in the number of progenitors subsequently leading a significant reduction in neuronal density and cortical thickness (Raballo et al.,

2000). In vitro studies, and the cortical phenotype of the Fgf2 knockout, suggests that it acts to expand the progenitor population, a function that would oppose that which our analysis of the Fgf10 knockout suggests for Fgf10.

Three related Fgfs are expressed within the CoP, Fgf8, 17 and 18, and any direct influence that they exert on cortical progenitors must be through their secretion and migration from the CoP. Fgf8 has been implicated in the proliferation and survival of cortical progenitors. Mice with lower levels of Fgf8 expression have a much smaller cortex (Storm et al., 2006), whereas overexpression of Fgf8 results in a substantial increase in size of the targeted brain structure (Crossley et al., 1996), including cortex, where focal overexpression of Fgf8 early in corticogenesis results in a local increase in cortical size (Fukuchi-Shimogori and Grove, 2001). Fgf8 has also been reported to increase the mitotic index of cortical progenitors in vitro (Borello et al., 2008) as well as control apoptosis among progenitors (Storm et al., 2003). Neither Fgf8, nor any Fgf, has been reported to affect RG differentiation. Thus, the available evidence indicates that Fgfs expressed in the CoP, and in particular Fgf8, have functions in corticogenesis that are distinct from those of Fgf10. Our findings indicate that Fgf10 does not influence the proliferative capacity of progenitors per se, as we detect no effect of the deletion of Fgf10 on cell cycle kinetics and cell death. In contrast to the other Fgfs that affect cortical size, our findings show that Fgf10 does so by regulating the timing of RG differentiation, and as a consequence, Fgf10 controls the length of an early phase of corticogenesis during which the size of the progenitor population is expanded by symmetric division of NCs prior to RG differentiation and the onset of neurogenesis. Subsequent to this phase regulated by Fgf10, RG progenitors exhibit normal proliferation kinetics, and the expanded size of rostral cortex, both radially and tangentially, is due to the increased number of progenitors. Our results are consistent with the finding of a modest increase in proliferating progenitors in Fgfr2 mutant mice (Ever et al., 2008).

Our findings that RG differentiation is delayed rather than prevented in the Fgf10 knockout indicates that Fgf10 is sufficient to direct the differentiation of RG, but that it is not required per se for RG to eventually differentiate; thus, other factors can eventually bring about RG differentiation in rostral cortex. To date, though, little is known about the mechanisms controlling this differentiation process, and few players in this process have been defined. Identified players in the differentiation of RG include Notch and its downstream target erbB2, expressed by progenitors (Patten et al., 2003; Schmid et al., 2003). How these components mesh with the function of Fgf10 is presently unclear. For example, our findings from the Fgf10 knockout indicate that Fgf10 promotes the differentiation of NCs into RG, whereas analysis of mice deficient for Notch or its signaling components suggest that Notch acts to maintain the progenitor state (Anthony et al., 2005). The function of Fgf10 in facilitating RG differentiation also seems to be distinct from that of the signaling of neuregulins through ErbB2 and ErbB4 to maintain RG identity. For instance, the intracellular domain of ErbB4 forms a complex with TAB2 and N-CoR that represses astrocyte markers and maintains RG identity (Sardi et al., 2006). Furthermore, re-induction of ErbB2 in astrocytes in adult brain is sufficient to induce BLBP expression characteristic of RG fate (Ghashghaei et al., 2007). Thus a function of ErbB-neuregulin signaling is to control the transition of RG to astrocytes by suppressing astroglia fate, whereas our findings show that a function of Fgf10 is to control the transition of NCs to RG by promoting RG fate.

Curiously, the delay that we observe in RG differentiation is biased for rostral cortex, although Fgf10 is more-or-less uniformly expressed over the rostral-caudal cortical axis. Thus, other factors operating in caudal cortex can compensate for the loss of Fgf10 and direct differentiation on a relatively normal time schedule. Potential candidates are the Wnts, which are expressed in the cortical hem, a patterning center positioned at the caudal and midline margins of the nascent cortex (Grove et al., 1998). Wnts are implicated because they regulate expression of

β-catenin, a canonical Wnt signaling component, which itself can regulate the symmetric versus asymmetric balance in the mode of cell divisions (Chenn and Walsh, 2002); however, Wnts, nor the Wnt pathway, have been implicated in RG differentiation per se.

Fgf10 functions at least in part through its high affinity receptor Fgfr2, which is expressed throughout the cortical VZ over the same period as Fgf10 (Maric et al., 2007). A recent in vitro study using antisense oligonucleotides to diminish expression of Fgfr1, r2 and r3 in cortical NCs shows that Fgfr2 promotes NC differentiation into RG, as well as other cell types, including intermediate states in progenitor differentiation (Maric et al., 2007). This result is consistent with our finding that Fgf10 controls differentiation of progenitor states at the step that naïve progenitors, i.e. NCs, differentiate into RG.

A prominent phenotype of Fgf10 −/− mice is the significant increase in the thickness of the cortical plate in the rostral half of cortex due at least in part to about a third more neurons in a radial traverse through the cortical plate, and a significant increase in the size of the cortical hemisphere, largely due to the preferential tangential expansion of rostral cortex. These increases are in turn due to an increased number of cortical progenitors due to the delay in the transition of NCs into differentiated RG and the resulting expansion of progenitors through the symmetric division of NCs. Models of corticogenesis suggest that early changes in symmetric cell divisions that expand the progenitor pool size would result in a increase in cortical surface area, whereas a later increase in asymmetric cell divisions to add neurons onto pre-existing columns would result selectively in an increase in cortical thickness (Caviness et al., 1995; Rakic, 1995).

As predicted by these models, we find that the increase in progenitors within rostral cortex does correlate with, and likely produces, the significant increase in the tangential area of rostral cortex in the Fgf10 mutant. However, we also find a significant increase in the radial thickness of cortical layers and the overall cortical plate in the Fgf10 mutant, but we do not find significant changes of cell cycle length, a mechanism proposed to increase asymmetric cell divisions by reducing cycle time and thereby increase the thickness of cortical layers (Caviness et al., 1995; Rakic, 1995). Indeed, mice deficient for the cell cycle inhibitor, p27, have increased radial thickness of the cortical plate whereas transgenic mice that overexpress p27 have reduced radial thickness, suggested to be due to altering the number of asymmetric cell divisions that produce a neuron by altering the length of the cell cycle (Caviness et al., 2003). Thus, a mechanism other than cell cycle control must be responsible for the increase in radial thickness of layers in Fgf10−/−cortex.

A likely mechanism is suggested by our finding of an increased number of progenitors in a radial traverse through the cortical wall. Based on the radial unit model and observations that neurons produced by progenitors migrate radially and stack upon one another to form radial columns (Kornack and Rakic, 1995; Luskin et al., 1988; Noctor et al., 2001), we would anticipate that an increase in progenitors, both RG and BPs, in a radial traverse would translate into a thicker "radial column" within the overlying cortical plate, as we observe for rostral cortex in the Fgf10 mutant. The increase in RG would result in a subsequent increased generation of deep layer neurons, as well as BPs, and the increase in BPs would result in an increased generation of superficial layer neurons (Sessa et al., 2008). Thus, the increase in radial thickness of rostral cortex is due to a delay in the differentiation of RG from NCs selectively in rostral cortex, resulting in an increase in the progenitor pool in the VZ and of BPs in the SVZ, which together lead to an increase in the production of cortical neurons.

An interesting issue is whether the mechanisms that generate layer-specific neuronal types are faithfully recapitulated within the expanded population of progenitors that generate the radially expanded rostral cortex. This issue cannot be fully addressed in the constitutive Fgf10 knockout

mouse because at the time the mice die at P0, proliferation is still ongoing and neurons are still migrating to the cortical plate. Nonetheless, we have obtained some insight into this issue by performing a preliminary analysis of laminar fate comparing wt and Fgf10−/− cortex using layer-specific markers (RORβ, Otx1 and Tbr1), along with Nissl-stained sections. We find that each marker is properly expressed in the Fgf10 null cortex and that the thickness of each layer and associated marker expression appears to be proportionally increased in a qualitatively equivalent manner. Thus, although neurogenesis is delayed in the Fgf10 mutant and the population of progenitors is increased, laminar specification appears to be retained in a proportionally normal fashion.

Our analyses using markers of area identity show that underlying the preferential tangential expansion of rostral cortex in the Fgf10 mutant is the selective expansion of a cortical field with the composite identity of frontal areas. In others words, frontal areas are disproportionately represented in the expanded Fgf10 deficient cortex in both absolute and relative size. This finding indicates that even the early generated neurons exhibit the expanded frontal area identities in the Fgf10 deficient cortex, indicating that the area identities of progenitors become fixed before they enter the neurogenic phase. Further, because area identities are not "recalibrated" proportionally across the cortical VZ to account for the expanded population of progenitors within rostral cortex of Fgf10 mutants, we conclude that area identities are already established and fixed within the progenitor population as the extended period of the lengthened expansion phase begins.

Our findings on the area patterning of the Fgf10 deficient cortex have potential implications for how cortical areas have evolved. The neocortex of each mammalian species has a distinct pattern of areas. From a phylogenic point of view, these distinct patterns are proposed to have evolved from the area template of a common ancestor (Krubitzer, 2007). The frontal lobe, to which many components of intelligence and higher level cognition have been attributed, is a cortical field that exhibits tremendous expansion over phylogeny, with a substantial leap in its expansion and specialization in the great apes and humans (Hill and Walsh, 2005). The genetic mechanisms responsible for such a disproportional expansion of frontal areas are unknown. However, our findings suggest a model in which alterations in the regulation of the transition period of NCs to RG by Fgf10, or other factors, and the concomitant overproduction of progenitors, both RG and BPs, can account for the selective expansion of specific cortical areas, such as the expansion of frontal areas seen in apes over evolution.

METHODS

Animals

Timed pregnant ICR mice and Fgf10 +/− mice (Min et al., 1998) were used in accordance with Institution guidelines. Fgf10 +/− mice were maintained on a C57BL/6 background. The day of insemination and the day of birth are designated as embryonic day 0.5 (E0.5) and postnatal day 0 (P0), respectively.

In situ hybridization

In situ hybridization was done using digoxigenin (DIG)-labeled riboprobes for Fgf8, Fgf10, Fgf17, Fgf18, ephrinA5 (image clone 4954342), Cad8, Lmo4, RORβ, Otx1 (image clone 6416436), and Tbr1, on whole brains or 20 μm cryostat sections as described previously (Sahara et al., 2007). In situ hybridization was done with the as described previously (Sahara et al., 2007). For in situ analysis of Fgf10, TSA Plus DNP system (Perkin Elmer) was used by following the manufacture's protocols.

In utero electroporation

Expression constructs of EGFP, Fgf10 was made by subcloning into pCAG vector and the surgery was done as described previously (Sahara et al., 2007).

Histochemistry

For immunostaining on sections, brains were fixed in 4% PFA in PBS, cryoprotected in 20% sucrose/PBS, cut at 20μm, and immunostained as described previously (Bishop et al., 2002). Dissociated cells were prepared by dissecting our the rostral half of cortices at indicated stages, treated with 0.2% trypsin for 5 min in HBSS, subsequently added DMEM containing 10% calf serum and dissociated by pipetting. Cells are fixed in 4% PFA immediately and centrifuge at 200 × g for 5 min in 24 well plates containing cover glasses, and immunostained. The following antibodies were used; rat anti-BrdU (Accurate), rabbit anti-cleaved caspase3 (Cell signaling), rabbit anti-Ki67 (Vector), rabbit anti-BLBP (Chemicon), guinea pig anti-GLAST (Chemicon), rabbit anti-Occludin (Zymed), rabbit anti-Tbr1 (Hevner et al., 2001), rabbit anti-Tbr2 (Chemicon), mouse anti-TuJ1 (Covance), mouse anti-Pax6 (Developmental Studies Hybridoma Bank). The size of cortex and areas were measured by NIH images software. Quantitative analyses of BLBP immunostaining intensity were done with NIH Image and Photoshop on images of four forebrain sections. Each photoimage was taken under the same conditions with a Q-Imaging Retiga-EX digital camera on a Nikon Microphot-FX microscope, imported into NIH Image as a grayscale eight-bit TIF. The dTel region was traced and digitally measured its size and intensity, and the "histogram" function in NIH Image was then used to generate a pixel and intensity count. Total intensity was determined by the number of pixels at each intensity multiplied by the actual intensity value of each pixel and summed; intensity levels from background pixels were subtracted from the total to yield signal intensity.

Determination of Cell cycle length

Cell cycle length was calculated by plotting of cumulative number of BrdU positive cells after 0.5, 1.5, and 4h of BrdU injection. Additional BrdU injection at 2h later was done for the data of 4h. At indicated time points, embryos are fixed in 4% PFA, cryoprotected in 20% sucrose, sectioned in 20 μm, and stained with anti-BrdU antibody.

Pair-cell analysis

Clonal culture and pair-cell analysis were done according to Qian et al (Qian et al., 1998). Briefly, the rostral half of cortices of wt or Fgf10 −/− embryos at E12.5 were dissected and dissociated in single clones as described (Qian et al., 1998). Single cells were plated in poly-L-lysine coated 60-well Terasaki plates or 8-well culture slides and incubated at 35°C, 6% CO2, and 100% humidity. Pair cells were identified after 24 h incubation by fixing with 4% PFA and stained with TuJ1 antibody and DAPI for nuclear staining.

Supplementary Material

Refer to Web version on PubMed Central for supplementary material.

ACKNOWLEDGEMENTS

We thank Todd McLaughlin and Chuck Stevens for comments on the manuscript, Yasuhiko Kawakami and Juan Carlos Belmonte for materials, Haydee Gutierrez and Berta Higgins for technical assistance, Scott Simonet for Fgf10 mutant mice, Robert Hevner for Tbr1 antibody, and Stephen Noctor and Arnold Kriegstein for sharing unpublished observations. This work was supported by NIH grants R37 NS31558 and R01 MH086147 (DDMO). SS was supported by fellowships from the JSPS Fellowships for Research Abroad and the Uehara Memorial Foundation.

REFERENCES

Aaku-Saraste E, Hellwig A, Huttner WB. Loss of Occludin and functional tight junctions, but not ZO-1, during neural tube closure--remodeling of the neuroepithelium prior to neurogenesis. Dev Biol 1996;180:664–679. [PubMed: 8954735]

Anthony TE, Klein C, Fishell G, Heintz N. Radial glia serve as neuronal progenitors in all regions of the central nervous system. Neuron 2004;41:881–890. [PubMed: 15046721]

Anthony TE, Mason HA, Gridley T, Fishell G, Heintz N. Brain lipid-binding protein is a direct target of Notch signaling in radial glial cells. Genes Dev 2005;19:1028–1033. [PubMed: 15879553]

Bachler M, Neubuser A. Expression of members of the Fgf family and their receptors during midfacial development. Mech Dev 2001;100:313–316. [PubMed: 11165488]

Bishop KM, Rubenstein JL, O'Leary DD. Distinct actions of Emx1, Emx2, and Pax6 in regulating the specification of areas in the developing neocortex. J Neurosci 2002;22:7627–7638. [PubMed: 12196586]

Borello U, Cobos I, Long JE, Murre C, Rubenstein JL. FGF15 promotes neurogenesis and opposes FGF8 function during neocortical development. Neural Develop 2008;3:17.

Bulchand S, Subramanian L, Tole S. Dynamic spatiotemporal expression of LIM genes and cofactors in the embryonic and postnatal cerebral cortex. Dev Dyn 2003;226:460–469. [PubMed: 12619132]

Caviness VS Jr, Goto T, Tarui T, Takahashi T, Bhide PG, Nowakowski RS. Cell output, cell cycle duration and neuronal specification: a model of integrated mechanisms of the neocortical proliferative process. Cereb Cortex 2003;13:592–598. [PubMed: 12764033]

Caviness VS Jr, Takahashi T, Nowakowski RS. Numbers, time and neocortical neuronogenesis: a general developmental and evolutionary model. Trends Neurosci 1995;18:379–383. [PubMed: 7482802]

Chenn A, Walsh CA. Regulation of cerebral cortical size by control of cell cycle exit in neural precursors. Science 2002;297:365–369. [PubMed: 12130776]

Cholfin JA, Rubenstein JL. Patterning of frontal cortex subdivisions by Fgf17. Proc Natl Acad Sci U S A 2007;104:7652–7657. [PubMed: 17442747]

Crossley PH, Martinez S, Martin GR. Midbrain development induced by FGF8 in the chick embryo. Nature 1996;380:66–68. [PubMed: 8598907]

Englund C, Fink A, Lau C, Pham D, Daza RA, Bulfone A, Kowalczyk T, Hevner RF. Pax6, Tbr2, and Tbr1 are expressed sequentially by radial glia, intermediate progenitor cells, and postmitotic neurons in developing neocortex. J Neurosci 2005;25:247–251. [PubMed: 15634788]

Ever L, Zhao RJ, Eswarakumar VP, Gaiano N. Fibroblast growth factor receptor 2 plays an essential role in telencephalic progenitors. Dev Neurosci 2008;30:306–318. [PubMed: 18073459]

Fukuchi-Shimogori T, Grove EA. Neocortex patterning by the secreted signaling molecule FGF8. Science 2001;294:1071–1074. [PubMed: 11567107]

Gaiano N, Nye JS, Fishell G. Radial glial identity is promoted by Notch1 signaling in the murine forebrain. Neuron 2000;26:395–404. [PubMed: 10839358]

Ghashghaei HT, Weimer JM, Schmid RS, Yokota Y, McCarthy KD, Popko B, Anton ES. Reinduction of ErbB2 in astrocytes promotes radial glial progenitor identity in adult cerebral cortex. Genes Dev 2007;21:3258–3271. [PubMed: 18079173]

Gotz M, Huttner WB. The cell biology of neurogenesis. Nat Rev Mol Cell Biol 2005;6:777–788. [PubMed: 16314867]

Grove EA, Tole S, Limon J, Yip L, Ragsdale CW. The hem of the embryonic cerebral cortex is defined by the expression of multiple Wnt genes and is compromised in Gli3-deficient mice. Development 1998;125:2315–2325. [PubMed: 9584130]

Gutin G, Fernandes M, Palazzolo L, Paek H, Yu K, Ornitz DM, McConnell SK, Hebert JM. FGF signalling generates ventral telencephalic cells independently of SHH. Development 2006;133:2937–2946. [PubMed: 16818446]

Hartfuss E, Galli R, Heins N, Gotz M. Characterization of CNS precursor subtypes and radial glia. Dev Biol 2001;229:15–30. [PubMed: 11133151]

Hevner RF, Shi L, Justice N, Hsueh Y, Sheng M, Smiga S, Bulfone A, Goffinet AM, Campagnoni AT, Rubenstein JL. Tbr1 regulates differentiation of the preplate and layer 6. Neuron 2001;29:353–366. [PubMed: 11239428]

Hill RS, Walsh CA. Molecular insights into human brain evolution. Nature 2005;437:64–67. [PubMed: 16136130]

Kornack DR, Rakic P. Radial and horizontal deployment of clonally related cells in the primate neocortex: relationship to distinct mitotic lineages. Neuron 1995;15:311–321. [PubMed: 7646888]

Krubitzer L. The magnificent compromise: cortical field evolution in mammals. Neuron 2007;56:201–208. [PubMed: 17964240]

Kuida K, Haydar TF, Kuan CY, Gu Y, Taya C, Karasuyama H, Su MS, Rakic P, Flavell RA. Reduced apoptosis and cytochrome c-mediated caspase activation in mice lacking caspase 9. Cell 1998;94:325–337. [PubMed: 9708735]

Kuida K, Zheng TS, Na S, Kuan C, Yang D, Karasuyama H, Rakic P, Flavell RA. Decreased apoptosis in the brain and premature lethality in CPP32-deficient mice. Nature 1996;384:368–372. [PubMed: 8934524]

Luskin MB, Pearlman AL, Sanes JR. Cell lineage in the cerebral cortex of the mouse studied in vivo and in vitro with a recombinant retrovirus. Neuron 1988;1:635–647. [PubMed: 3272182]

Mackarehtschian K, Lau CK, Caras I, McConnell SK. Regional differences in the developing cerebral cortex revealed by ephrin-A5 expression. Cereb Cortex 1999;9:601–610. [PubMed: 10498278]

Malatesta P, Hack MA, Hartfuss E, Kettenmann H, Klinkert W, Kirchhoff F, Gotz M. Neuronal or glial progeny: regional differences in radial glia fate. Neuron 2003;37:751–764. [PubMed: 12628166]

Maric D, Fiorio Pla A, Chang YH, Barker JL. Self-renewing and differentiating properties of cortical neural stem cells are selectively regulated by basic fibroblast growth factor (FGF) signaling via specific FGF receptors. J Neurosci 2007;27:1836–1852. [PubMed: 17314281]

Min H, Danilenko DM, Scully SA, Bolon B, Ring BD, Tarpley JE, DeRose M, Simonet WS. Fgf-10 is required for both limb and lung development and exhibits striking functional similarity to Drosophila branchless. Genes Dev 1998;12:3156–3161. [PubMed: 9784490]

Murphy M, Drago J, Bartlett PF. Fibroblast growth factor stimulates the proliferation and differentiation of neural precursor cells in vitro. J Neurosci Res 1990;25:463–475. [PubMed: 2112611]

Noctor SC, Flint AC, Weissman TA, Dammerman RS, Kriegstein AR. Neurons derived from radial glial cells establish radial units in neocortex. Nature 2001;409:714–720. [PubMed: 11217860]

O'Leary DD, Chou SJ, Sahara S. Area patterning of the mammalian cortex. Neuron 2007;56:252–269. [PubMed: 17964244]

Ornitz DM, Xu J, Colvin JS, McEwen DG, MacArthur CA, Coulier F, Gao G, Goldfarb M. Receptor specificity of the fibroblast growth factor family. J Biol Chem 1996;271:15292–15297. [PubMed: 8663044]

Patten BA, Peyrin JM, Weinmaster G, Corfas G. Sequential signaling through Notch1 and erbB receptors mediates radial glia differentiation. J Neurosci 2003;23:6132–6140. [PubMed: 12853432]

Qian X, Goderie SK, Shen Q, Stern JH, Temple S. Intrinsic programs of patterned cell lineages in isolated vertebrate CNS ventricular zone cells. Development 1998;125:3143–3152. [PubMed: 9671587]

Raballo R, Rhee J, Lyn-Cook R, Leckman JF, Schwartz ML, Vaccarino FM. Basic fibroblast growth factor (Fgf2) is necessary for cell proliferation and neurogenesis in the developing cerebral cortex. J Neurosci 2000;20:5012–5023. [PubMed: 10864959]

Rakic P. A small step for the cell, a giant leap for mankind: a hypothesis of neocortical expansion during evolution. Trends Neurosci 1995;18:383–388. [PubMed: 7482803]

Sahara S, Kawakami Y, Izpisua Belmonte JC, O'Leary D. Sp8 exhibits reciprocal induction with Fgf8 but has an opposing effect on anterior-posterior cortical area patterning. Neural Develop 2007;2:10.

Sardi SP, Murtie J, Koirala S, Patten BA, Corfas G. Presenilin-dependent ErbB4 nuclear signaling regulates the timing of astrogenesis in the developing brain. Cell 2006;127:185–197. [PubMed: 17018285]

Schmid RS, McGrath B, Berechid BE, Boyles B, Marchionni M, Sestan N, Anton ES. Neuregulin 1-erbB2 signaling is required for the establishment of radial glia and their transformation into astrocytes in cerebral cortex. Proc Natl Acad Sci U S A 2003;100:4251–4256. [PubMed: 12649319]

Sessa A, Mao CA, Hadjantonakis AK, Klein WH, Broccoli V. Tbr2 directs conversion of radial glia into basal precursors and guides neuronal amplification by indirect neurogenesis in the developing neocortex. Neuron 2008;60:56–69. [PubMed: 18940588]

Storm EE, Garel S, Borello U, Hebert JM, Martinez S, McConnell SK, Martin GR, Rubenstein JL. Dose-dependent functions of Fgf8 in regulating telencephalic patterning centers. Development 2006;133:1831–1844. [PubMed: 16613831]

Storm EE, Rubenstein JL, Martin GR. Dosage of Fgf8 determines whether cell survival is positively or negatively regulated in the developing forebrain. Proc Natl Acad Sci U S A 2003;100:1757–1762. [PubMed: 12574514]

Suzuki SC, Inoue T, Kimura Y, Tanaka T, Takeichi M. Neuronal circuits are subdivided by differential expression of type-II classic cadherins in postnatal mouse brains. Mol Cell Neurosci 1997;9:433–447. [PubMed: 9361280]

Takahashi T, Goto T, Miyama S, Nowakowski RS, Caviness VS Jr. Sequence of neuron origin and neocortical laminar fate: relation to cell cycle of origin in the developing murine cerebral wall. J Neurosci 1999;19:10357–10371. [PubMed: 10575033]

Treier M, O'Connell S, Gleiberman A, Price J, Szeto DP, Burgess R, Chuang PT, McMahon AP, Rosenfeld MG. Hedgehog signaling is required for pituitary gland development. Development 2001;128:377–386. [PubMed: 11152636]

Vaccarino FM, Schwartz ML, Raballo R, Nilsen J, Rhee J, Zhou M, Doetschman T, Coffin JD, Wyland JJ, Hung YT. Changes in cerebral cortex size are governed by fibroblast growth factor during embryogenesis. Nat Neurosci 1999;2:246–253. [PubMed: 10195217]

Yoon K, Nery S, Rutlin ML, Radtke F, Fishell G, Gaiano N. Fibroblast growth factor receptor signaling promotes radial glial identity and interacts with Notch1 signaling in telencephalic progenitors. J Neurosci 2004;24:9497–9506. [PubMed: 15509736]

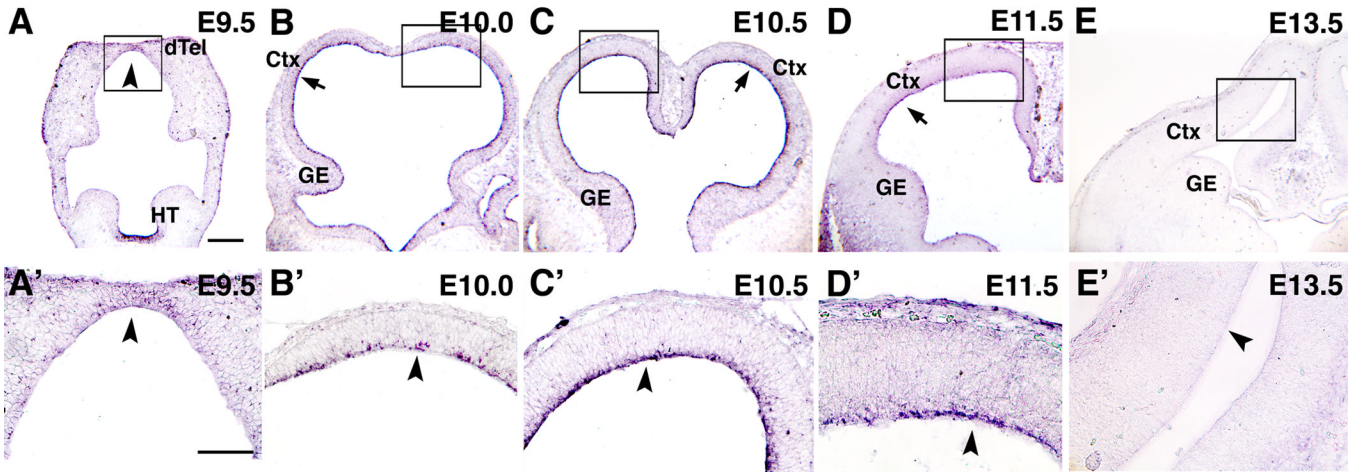

Figure 1. Transient expression of Fgf10 at apical aspect of cortical VZ

Tangential (A, A'), and coronal (B–E, B'–E') sections from wt brains processed for in situ hybridization using DIG-Fgf10 probes at ages indicated. Boxed areas in A–E are shown at higher magnification in A'–E'. At E9.5 (A, A'), Fgf10 expression is robust in hypothalamus, but is not detectable in dTel, other than very weak expression near rostral midline (arrowhead). Strong Fgf10 expression is detected at apical surface of dTel (arrow in B–D; arrowhead in B'–D') at E10.0 (B, B') and E10.5 (C, C'), and is sustained at E11.5 (D, D'), but downregulated to non-detectable by E13.5 (E, arrow; E', arrowhead). Scale bars: 0.2 mm (A–E), 0.1 mm (A'–E'). dTel: dorsal telencephalon, HT: hypothalamus, Ctx: cortex, GE, ganglionic eminence.

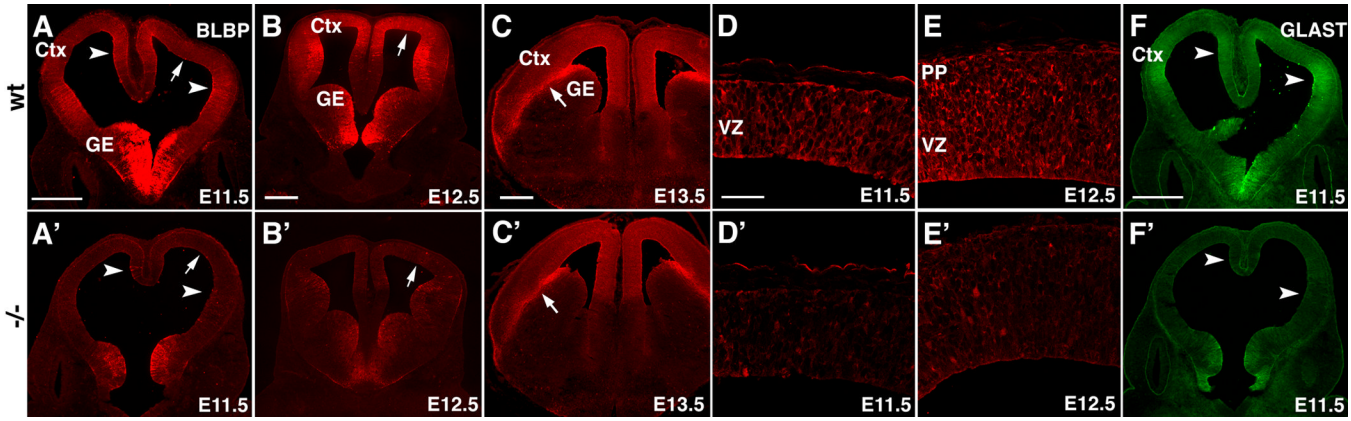

Figure 2. Loss of Fgf10 delays radial glia differentiation

(A–F') Immunofluorescence staining of wt (wt) (A–F) and Fgf10 −/− (A'–F') brains at ages indicated with antibodies against radial glia markers, BLBP (A–E') and GLAST (F, F'). At E11.5 in wt, stronger staining for BLBP and GLAST was detected in medial and ventrolateral cortex (arrowheads in A, F) and moderate staining elsewhere in cortex (arrow). Same staining pattern is evident at E12.5, but overall staining levels are higher (B). By E13.5, staining becomes relatively high throughout cortex, and the radial glia fibers emanating from the pallial-subpallial boundary are particularly intensely labeled (arrow in C). Compared to wt, in the Fgf10 −/− cortex, BLBP staining (A', B') and GLAST staining (F') is substantially diminished. By E13.5, staining is comparable between wt (C) and Fgf10 −/− cortex (C'). Arrowheads and arrows mark same relative positions in Fgf10 −/− cortex (A'–C') as in wt cortex (A–C). Moderate BLBP staining in mid cortex of wt at E11.5 and E12.5 (arrow in A, B, respectively) is shown at higher magnification in D and E. Diminished BLBP staining in mid cortex of Fgf10 −/− cortex at E11.5 and E12.5 (arrow in A', B', respectively) is shown at higher magnification in D' and E'. Scale bars: 0.5 mm (A, A'), 0.5 mm (B, B'), 0.5 mm(C, C'), 50 μm (D–F'), 0.5 mm (F, F'). Ctx: cortex, GE, ganglionic eminence, VZ ventricular zone, PP: preplate.

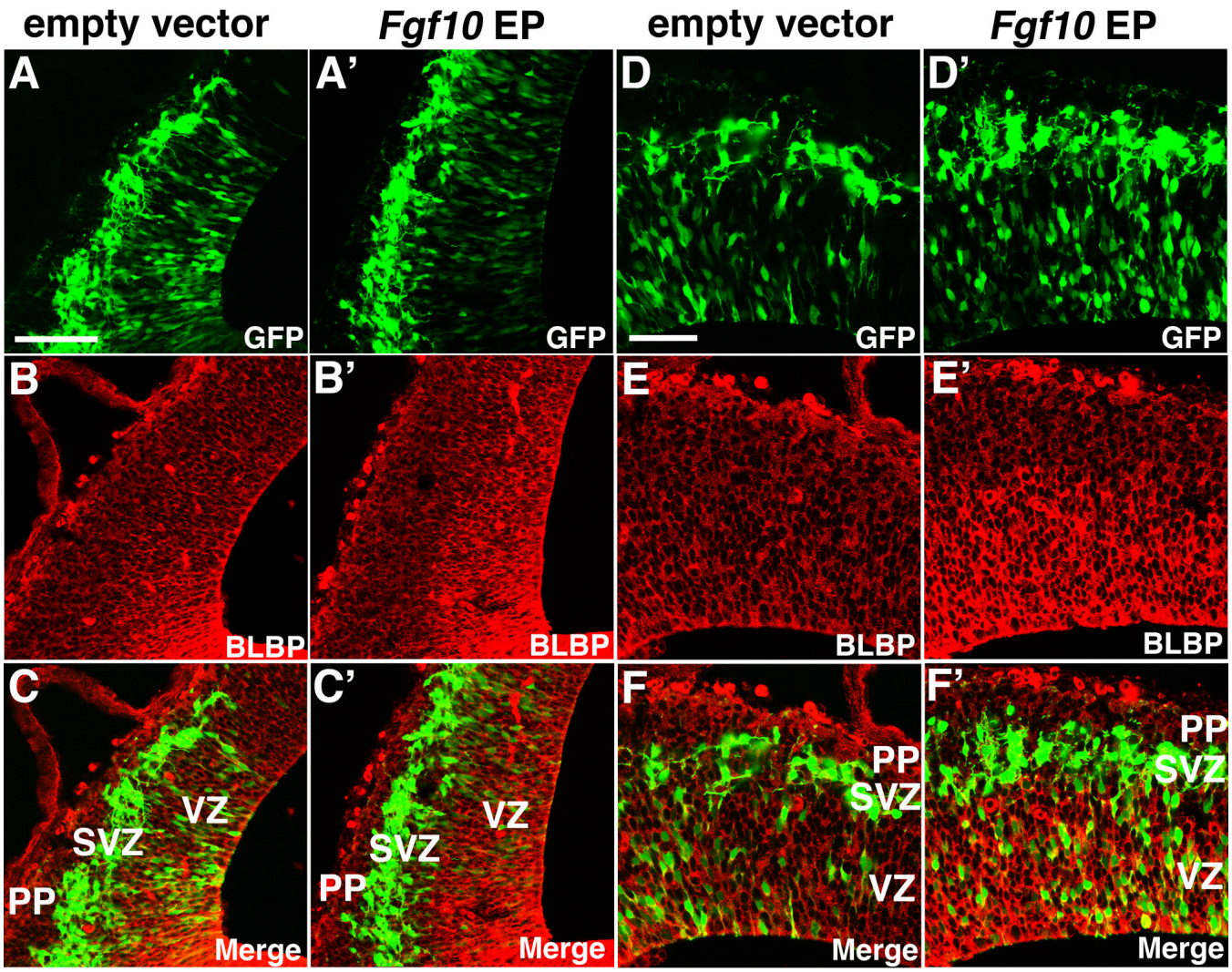

Figure 3. Fgf10 promotes radial glia differentiation in vivo

Fgf10 expression construct or empty vector was co-electroporated at E11.5 with an eGFP expression vector to confirm site, and BLBP staining was assessed at E12.5 on coronal sections. (A–C) Sections of E12.5 brains electroporated with empty vector at E11.5, stained with anti-BLBP antibody, exhibit staining similar to non-electroporated wt (not shown) (n=3): eGFP labeling reveals electroporation site; (B) BLBP immunostaining; (C) merged image. (A'–C') Sections of E12.5 brains electroporated with Fgf10 expression vector at E11.5, stained with anti-BLBP antibody, exhibit enhanced staining compared to empty vector cases (n=4): (A') eGFP labeling reveals electroporation site; (B') BLBP immunostaining; (C') merged image. Higher magnification images of empty vector-transfected cases shown in A–C and Fgf10-transfected cases shown in A'–C' are shown in D–F and D'–F', respectively. Scale bars: 0.1 mm (A–C'), 50 μm (D'–F'). VZ, ventricular zone; PP, preplate; SVZ, subventricular zone.

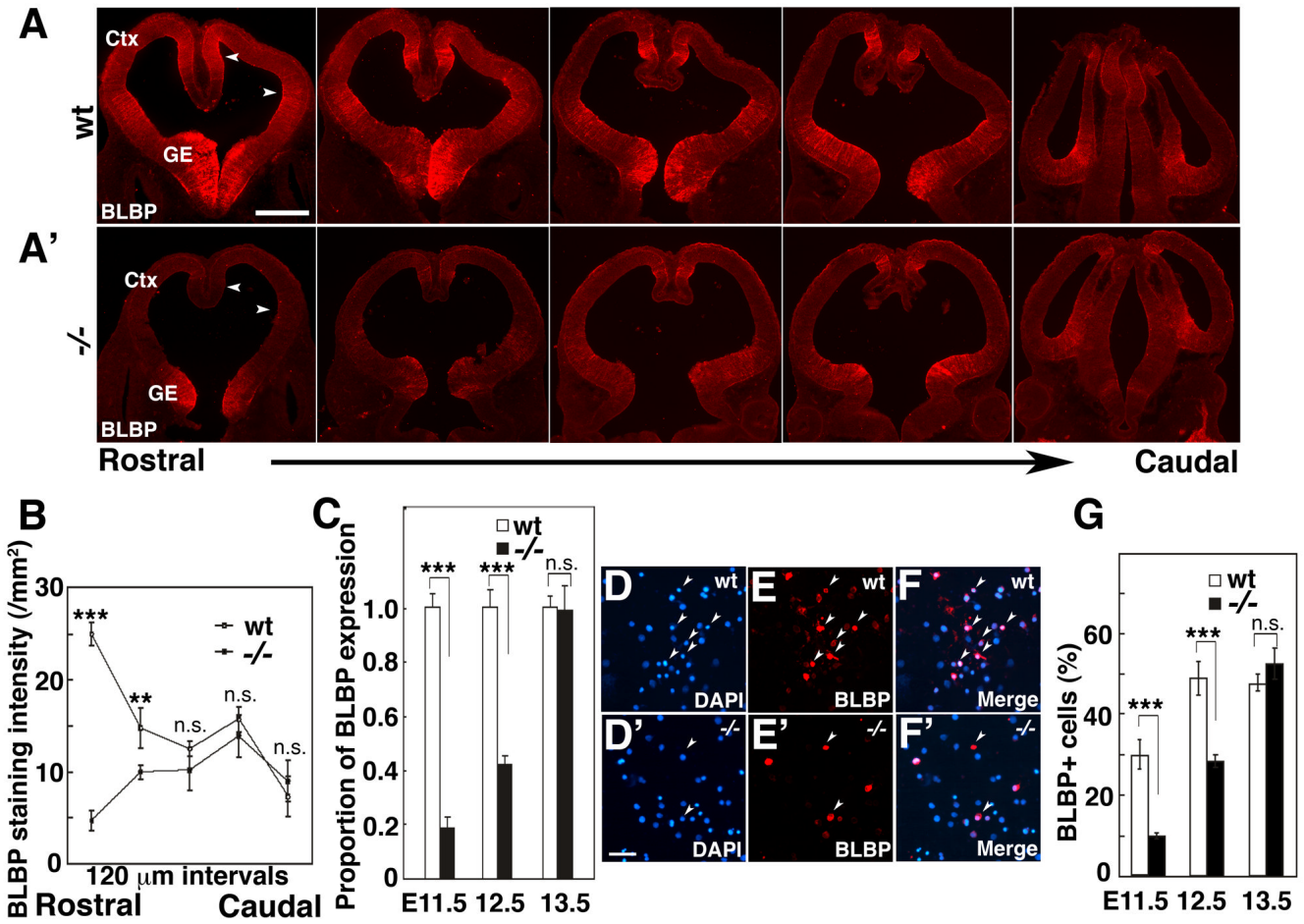

Figure 4. Loss of Fgf10 delays radial glia differentiation preferentially in rostral cortex

(A,A') BLBP immunostaining of series of coronal sections along rostral-caudal axis of wt (wt) (A) and Fgf10 −/− cortex (A'). (B) Quantification of BLBP staining intensity of wt and Fgf10 −/− cortices (n=4); mean ± s.e.m. is plotted at 120 μm intervals along the rostral-caudal cortical axis. BLBP staining is significantly diminished in rostral sections of Fgf10 −/− cortex compared to wt, but staining is comparable in caudal sections (also compare A to A') (Actual data for each plotted point in B, Rostral to Caudal and signifcanace, unpaired Student's t-test: wt 24.8 ± 2.3, KO 4.8 1.8, p<0.001; wt 14.8 ± 3.5, 9.9 ± 1.1, p< 0.01; 12.9 ± 1.4, 10.2 ± 3.4, n.s.; 16.7 ± 2.1, 13.8 ± 2.9, n.s.; 8.2 ± 3.4, 7.2 ± 3.0, n.s.) (C) Fluorescence intensity of BLBP staining in rostral cortex at E11.5, E12.5 and E13.5 in wt and Fgf10 −/− mice (n=4, 1.0 ± 0.051 s.e.m. at E11.5,1.0 ± 0.064 s.e.m. at E12.5, 1.0 ± 0.041 s.e.m. at E13.5 for wt, and 0.18 ± 0.038 s.e.m. at E11.5, 0.48 ± 0.028 s.e.m. at E12.5, 0.99 ± 0.09 s.e.m. at E13.5 for Fgf10 −/−, respectively. Significance between wt and Fgf10 −/−mice in unpaired Student's test is p<0.001 at E11.5, p<0.001 at E12.5, and n.s. at E13.5). The difference in BLBP expression between wt and Fgf10 −/− rostral cortex is substantial at E11.5 and E12.5, but is indistinguishable at E13.5; thus, the delay in upregulation of BLBP expression in Fgf10 −/− cortex is transient. (D–F) Quantification of BLBP positive cells in rostral cortex of wt or Fgf10 −/− littermates. Dissociated cells from E11.5 rostral cortex of wt (D, E, F) or Fgf10 −/− (D', E', F') were immunostained by BLBP antibody (E, E') and counterstained with DAPI (D, D'). Merged images are shown in F and F'. (G) Total cells of E11.5, E12.5 and E13.5 stained by DAPI and positive cells for BLBP staining were counted, respectively (three independent experiments, 10 fields examined per experiment, 29.7 ± 3.6% s.e.m. at E11.5, 48.8 ± 4.0 % s.e.m. at E12.5,

69.5 ± 2.9 % s.e.m. at E13.5 for wt, 9.7 ± 0.8 % s.e.m. at E11.5, 28.2 ± 1.6 % s.e.m. at E12.5, 64.0 ± 2.3 % s.e.m. at E13.5 for Fgf10 −/−, respectively. Significance between wt and Fgf10 −/− mice in unpaired Student's test is $p<0.001$ at E11.5, $p<0.001$ at E12.5, and n.s. at E13.5). Scale bar: 0.5mm (A–E"), 0.1mm (D–F'). Ctx: cortex, GE: ganglionic eminence.

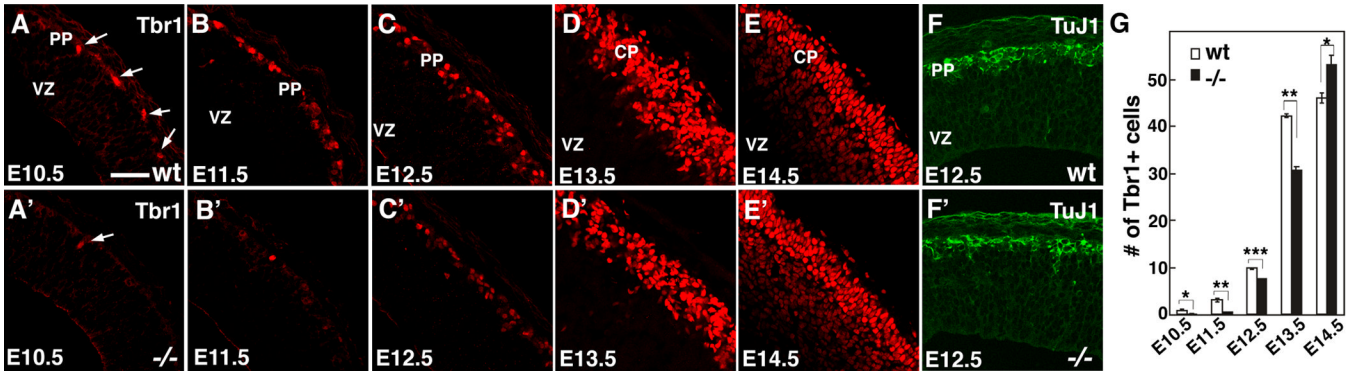

Figure 5. Fgf10 deletion delays onset of cortical neurogenesis with initially diminished neuronal production followed by enhanced production

(A–G) Early neurogenesis in wt and Fgf10 −/− cortex. Sections of wt (A–F) and Fgf10−/− (A'–F') brains at ages indicated were stained with a preplate and layer 6 marker, Tbr1 antibody (A–E'), or a pan-neuronal marker, TuJ1 (F, F'). At E10.5, a low density of Tbr1+ neurons (arrows) is evident in the preplate (PP) on each section through wt cortex (A), but only one neuron (arrow), or more typically, none are found in each section in Fgf10 −/− cortex (A'). From E10.5 through E13.5, fewer Tbr1+ neurons are evident in Fgf10−/− cortex than in wt (A–E'), with a delay of approximately one and a half to two days in neuronal production; however, by E14.5, more neurons are found in cortical plate (CP) of Fgf10 −/− cortex than wt (E, E'). (F, F') Tuj1 immunostaining also reveals lower density of preplate neurons in Fgf10 −/− cortex than wt. (G) Quantification of Tbr1+ neurons. (n=4, 0.85 ± 0.16 /0.01mm^2 s.e.m. at E11.5, 2.98 ± 0.31/0.01 mm^2 s.e.m. at E12.5, 9.78 ± 0.16 /0.01mm^2 s.e.m. at E13.5, 42.1 ± 0.47 /0.01mm^2 s.e.m. at E14.5, 45.9 ± 1.04 /0.01mm^2 s.e.m. at E15.5 for wt, 0.14 ± 0.04 / mm^2 s.e.m. at E11.5, 0.57 ± 0.01 mm^2 s.e.m. at E12.5, 7.37 ± 0.17 /0.01mm^2 s.e.m. at E13.5, 30.5 ± 0.75 /0.01mm^2 s.e.m. at E14.5, 52.9 ± 2.1 /0.01mm^2 s.e.m. at E15.5 for Fgf10−/−, respectively. Significance between wt and Fgf10−/− mice in unpaired Student's test is $p<0.05$ at E10.5, $p<0.01$ at E11.5, $p<0.001$ at E12.5, $p<0.01$ at E13.5, and $p<0.05$ at E14.5). VZ ventricular zone. Scale bar: 50 μm.

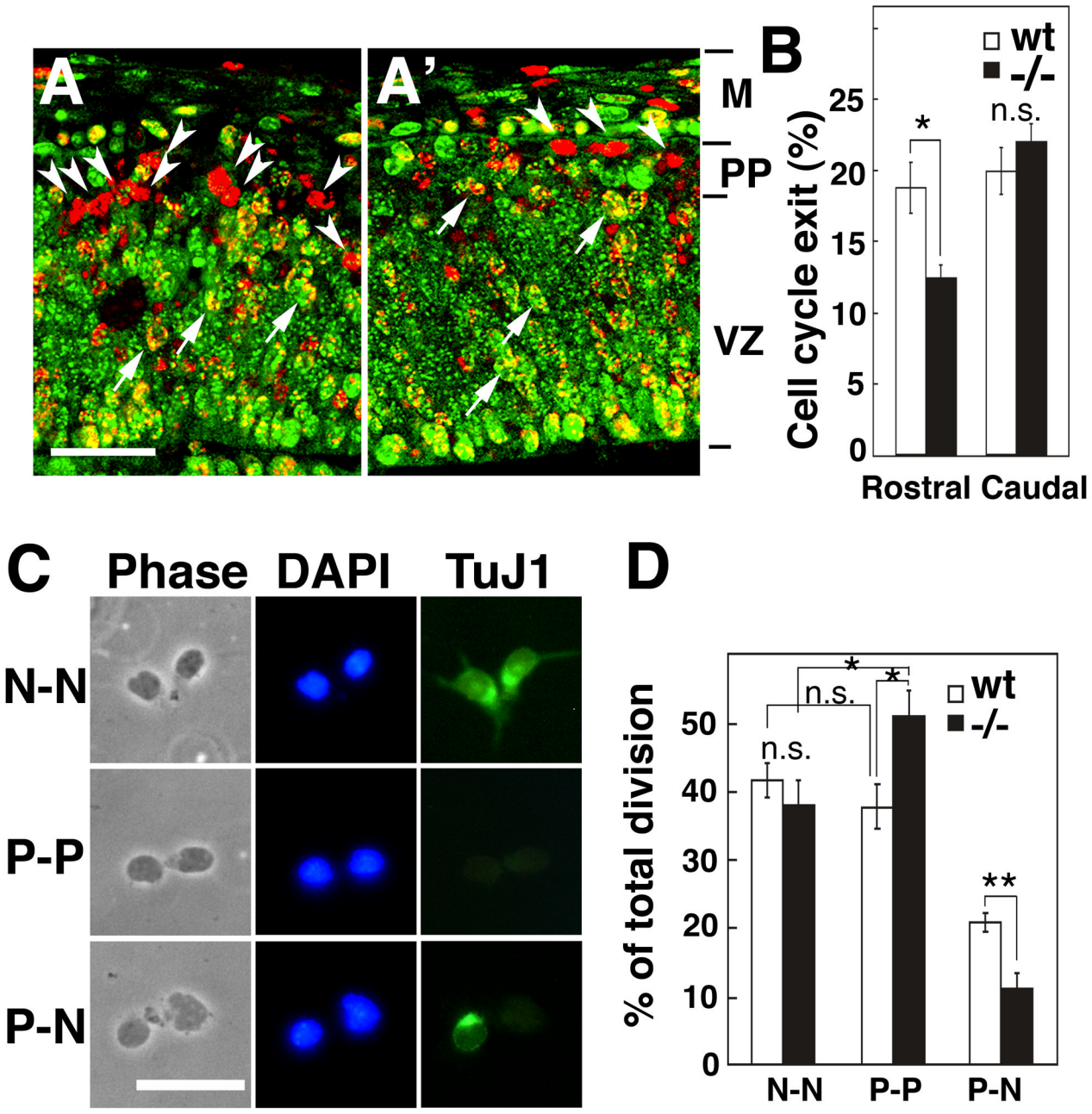

Figure 6. Delayed radial glia differentiation results in greater percentage of progenitors undergoing symmetric division producing two progenitors

(A–B) Cell cycle exit of early cortical progenitors in Fgf10−/− cortex. BrdU was injected into pregnant females at E11.5 and embryos were collected 24 hrs later at E12.5. Sections of E12.5 brains of wt (A) or Fgf10−/− (A') stained with BrdU antibody (red) and Ki67 antibody (green); examples of double labeled cells (arrows) and cells single labeled with BrdU (arrowheads) are marked. (B) Fewer cells leave cell cycle in Fgf10 −/− cortex than in wt. Percentage exit was calculated by dividing number of cells single labeled by BrdU by total number of cells single labeled by BrdU and double labeled by Ki67 in addition. Abut 34% fewer cells exit the proliferative cell cycle in rostral Fgf10 −/− cortex than wt (n=4, 18.7 ± 1.80% s.e.m. for wt, 12.4 ± 0.86% s.e.m., $p<0.05$ for −/−), whereas exit in caudal cortex is indistinguishable (B,

n=4, 19.9 ± 1.60% s.e.m. for wt, 22.0 ± 1.27% s.e.m. for −/−). Abbreviations: M, meninges; PP, preplate; VZ, ventricular zone. (C–D) Pair-cell analysis of wt and Fgf10−/− cortex in vitro. (C) Output of divisions by cortical progenitors in clonal culture. Rostral halves of cortices from wt or Fgf10 −/− embryos at E12.5 were dissected, dissociated, plated at clonal density, followed for 24 hours in culture, and then immunostained with TuJ1 antibody. Shown are pairs of progeny from progenitor division: phase contrast image, DAPI staining (blue), and TuJ1 staining (green). Examples of three types of progeny pairs are shown: neuronal pairs (N-N, upper panels) generated by terminal symmetric division, progenitor pairs (P-P, middle panels) generated by expansion symmetric division, or neuron-progenitor pairs (N-P, lower panels) generated by asymmetric division. (D) In Fgf10−/− clones, P-P pairs are increased (n= 351, 38.7 ± 2.96% s.e.m. for wt, n= 251, 49.5 ± 5.1 s.e.m. for Fgf10 −/−, from three independent experiments, $P<0.05$) and P-N pairs are reduced (20.7 ± 0.56% SEM for wt, 11.7 ± 2.1 % s.e.m. for Fgf10 −/−, $p<0.01$) compared to wt, but N-N pairs are not significantly different (40.6 ± 2.4% s.e.m. for wt, 38.8 ± 4.9 % s.e.m. for Fgf10 −/−). Thus, compared to wt, 35% more progenitors from Fgf10 −/−cortex produce a pair of progenitors by symmetric division ($p<0.05$), whereas 47% fewer produce a progenitor and a neuron by asymmetric division ($p<0.01$), with no difference between wt and Fgf10−/− progenitors that produce two neurons by symmetric division (Figure 6D, n=351 pairs for wt, n=251 pairs for Fgf10−/−). Scale bars: 25 μm (A, A'), 20 μm (C). *$p<0.05$; **$p<0.01$, compared to wt by unpaired Student's t test.

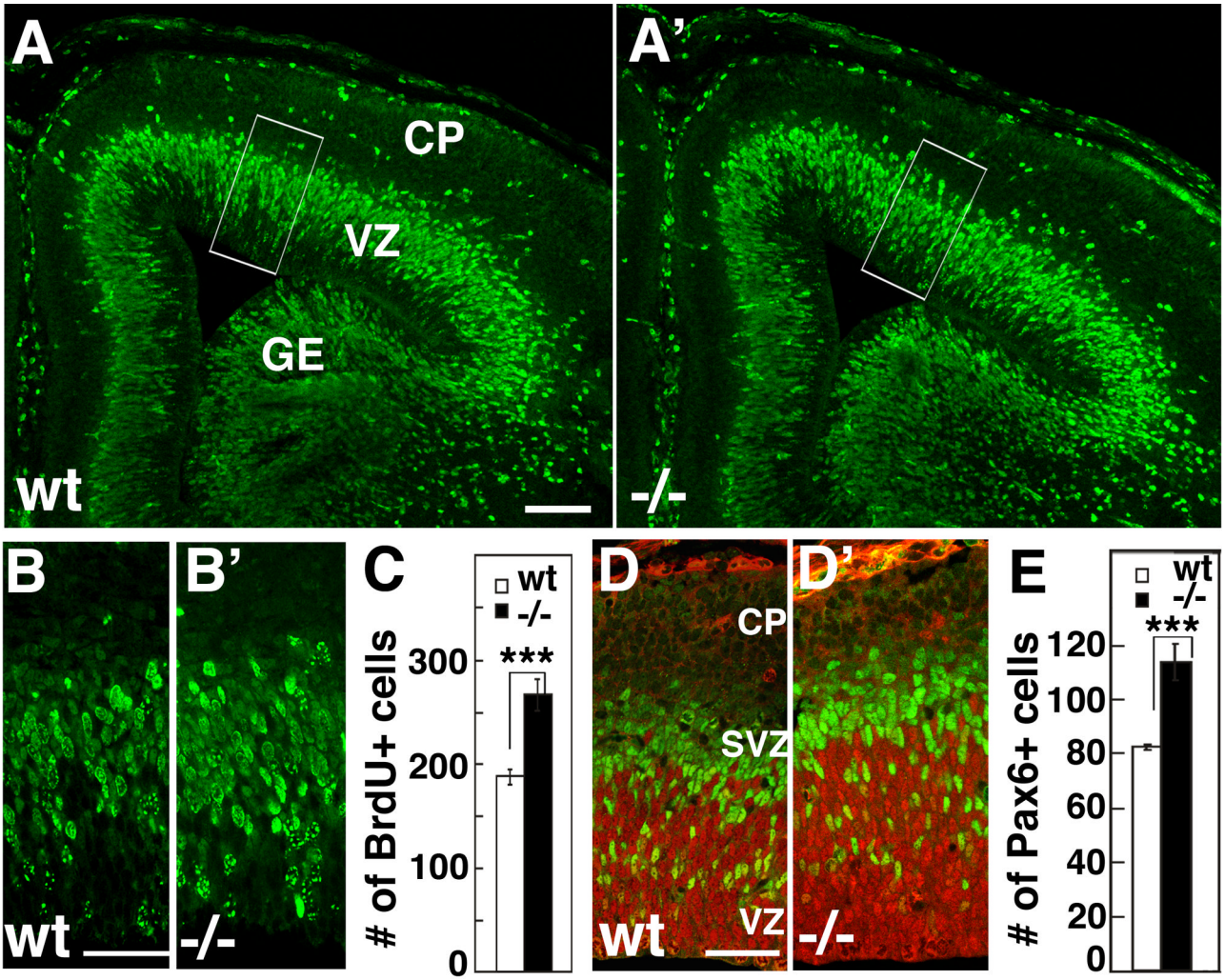

Figure 7. Fgf10 −/− cortex has significantly more progenitors in radial column than wild type cortex

Short-pulse BrdU labeling of wt and Fgf10−/− cortex at E14.5. BrdU was injected to pregnant females and E14.5 embryos were collected after 1 hour, and coronal sections through cortex were immunostained with anti-BrdU antibody. (A–B') More BrdU+ cells are evident in a radial traverse through Fgf10−/− cortex (A', B') than in wt (A, B). B and B' are higher power of boxed areas in A and A'. (C) Counts of BrdU positive cells in a 100 μm wide radial traverse across 20 μm thick sections (n=4, 187 ± 7.9 s.e.m. for wt, 265 ± 15.3 s.e.m. for Fgf10 −/−, unpaired Student's test, $p<0.001$ for both). (D, D') Double immunostaining of E14.5 wt and Fgf10 −/− rostral cortex with Pax6 antibody (red) specific for radial glia and Tbr2 antibody (green) specific for basal progenitors. (E) Counts of Pax6+ cells showing a significant increase in Fgf10 −/− rostral cortex compared to wt ($p<0.001$). VZ ventricular zone, SVZ subventricular zone, CP: cortical plate. Scale bars: 0.1 mm (A, A'), 20 μm (B, B'), 20 μm (D, D').

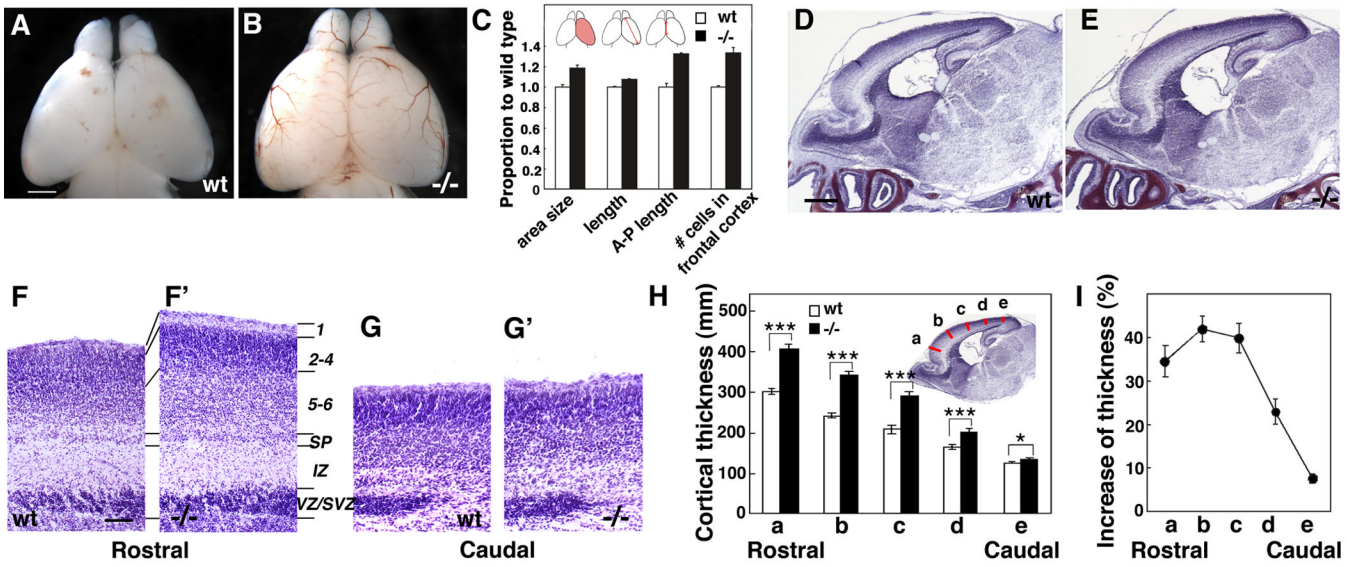

Figure 8. Fgf10 −/− mice exhibit overall increase in cortical surface area and increased laminar thickness preferentially in rostral cortex

(A, B) Dorsal views of P0 brains of wt (A) and Fgf10−/− mice (B). (C) Quantitative comparison of brain size between wt (n=4) and Fgf10 −/− mice (n=4) at P0. Area size: dorsal cortical surface area is 18.6 ± 2.93 % greater in Fgf10 −/− than wt; length from the top of the rostral pole to the caudolateral pole is 7.3% ± 0.88% greater in Fgf10 −/− than wt; length of midline structure across anterior/posterior axis is 32.4 ± 9.45% greater in Fgf10 −/− than wt; number of cells in a 100 μm wide radial traverse in 20 μm thick sections in rostral cortex is 34% ± 4.8% greater in Fgf10 −/− than wt. (D, E) Nissl staining of sagittal sections of P0 brain of wt (D) and Fgf10−/− mice (E). Rostral cortex is significantly thicker in Fgf10 −/− mice than in wt. (F – G') Higher power views of Nissl stained sections through rostral and caudal cortex of wt and Fgf10 −/− mice. Laminar patterning in Fgf10 −/− cortex resembles wt, but the cellular layers are thicker in Fgf10 −/− rostral cortex compared to wt; no difference is evident between wt and Fgf10 −/− caudal cortex. (H) Quantification of cortical laminar thickness. Measurement were done at five different position as indicated (a to e) of the radial thickness from bottom of the subplate to the pial surface. (I) Percentage increase of cortical radial thickness in Fgf10−/− cortex compared to wt (Student's test; $p<0.001$ for position a to d, and $p<0.01$ for e). Scale bars: 0.5 mm (A. B), 0.5 mm (D, E), 0.1 mm (F–G').

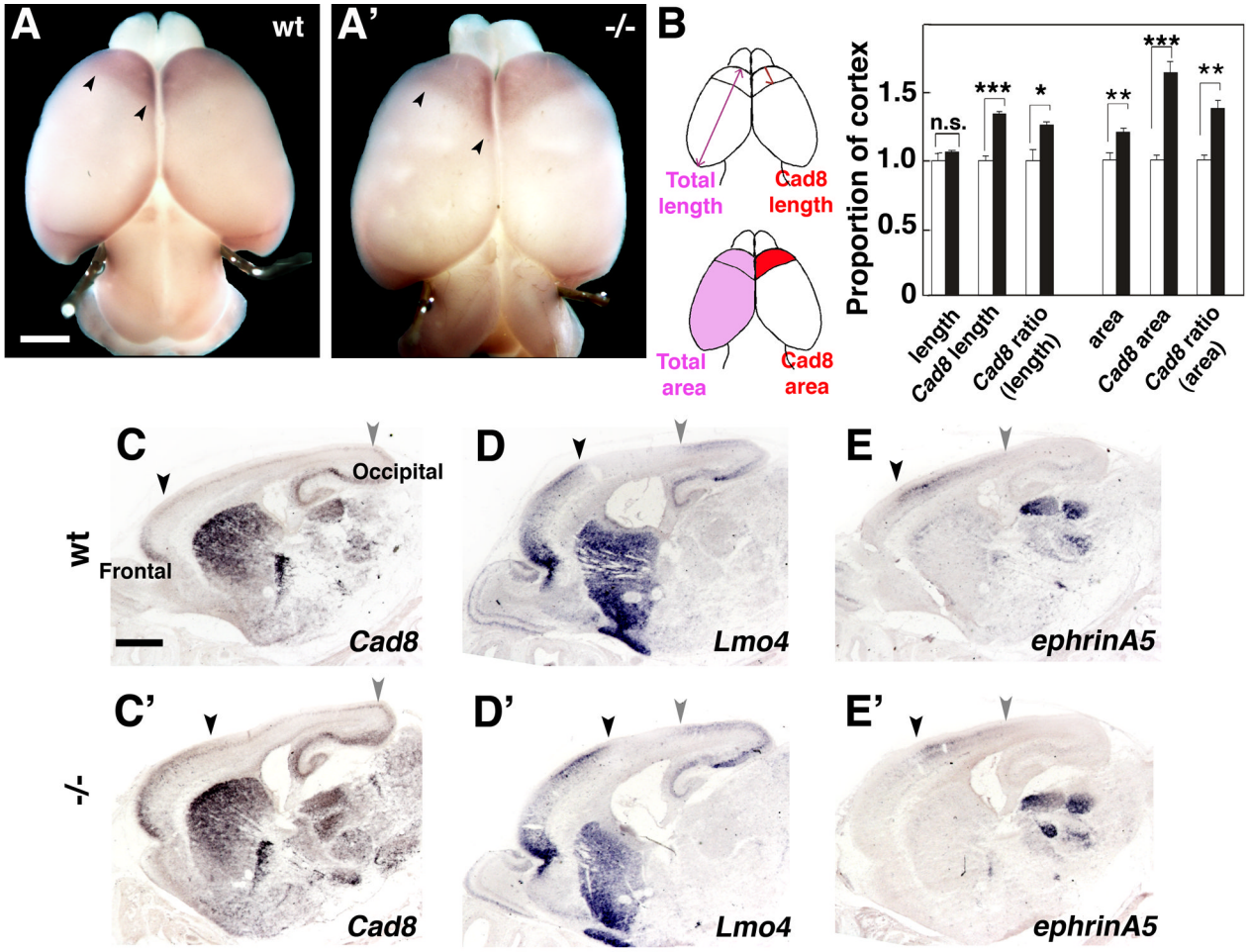

Figure 9. Frontal areas are preferentially expanded in Fgf10 −/− cortex

(A, A') Dorsal views of P0 brains of wt (A) or Fgf10−/− (A') mice processed for whole mount in situ hybridization with DIG-labeled cad8 riboprobes. (B) Quantification of the frontal cad8 expression domain in wt or Fgf10−/− cortex as indicated in drawing. Both absolute and relative areas and lengths, for both overall and Cad8 domain measurements, are increased in the Fgf10 −/− cortex compared to wt: Overall area, 12.0 ± 4.0%, unpaired Student's t-test, n.s.; Overall length, 6.36 ± 4.8%, n.s.. Cad8 domains: Absolute sizes (64.0 ± 3.1% increase for area, $p<0.001$; 34.0 ± 3.0% for length, $p<0.001$), Relative sizes / corrected for overall (36.9 ± 2.6% increase for area, $p<0.01$; 26.0 ± 2.8% increase for length, $p<0.05$). (C–E') In situ hybridization analysis of sagittal sections of P0 wt and Fgf10 −/− brains with cad8, Lmo4, and ephrin-A5, as indicated. Black arrowheads mark the caudal border of the frontal expression domain of cad8 (C,C') and Lmo4 (D,D'), and the rostral border of the mid-cortex expression domain of ephrin-A5. The gray arrowheads mark the rostral border of the occipital expression domain of cad8 (C,C') and Lmo4 (D,D'), and the caudal border of the mid-cortex expression domain of ephrin-A5. Scale bars: 0.5mm (A, A'), 0.5 mm (C–D').